J. Cell. Mol. Med. Vol 16, No 11, 2012 pp. 2813-2826

Topical application of phosphatidyl-inositol-3,5-bisphosphate for acute lung injury in neonatal swine

Stefanie Preuß [a], Friede D. Omam [a], Julia Scheiermann [a], Sabrina Stadelmann [a], Supandi Winoto-Morbach [b], Philipp von Bismarck [a], Sabine Adam-Klages [b], Friederike Knerlich-Lukoschus [c], Dennis Lex [d], Daniela Wesch [b], Janka Held-Feindt [c], Stefan Uhlig [d], Stefan Schütze [b], Martin F. Krause [a, *]

[a] *Universitätsklinikum Schleswig-Holstein, Campus Kiel, Department of Pediatrics, Kiel, Germany*
[b] *Universitätsklinikum Schleswig-Holstein, Campus Kiel, Institute of Immunology, Kiel, Germany*
[c] *Universitätsklinikum Schleswig-Holstein, Campus Kiel, Department of Neurosurgery, Kiel, Germany*
[d] *Universitätsklinikum, RWTH Aachen, Institute of Pharmacology and Toxicology, Aachen, Germany*

Received: June 1, 2012; Accepted: August 3, 2012

Abstract

Hypoxemic respiratory failure of the neonatal organism involves increased acid sphingomyelinase (aSMase) activity and production of ceramide, a second messenger of a pro-inflammatory pathway that promotes increased vascular permeability, surfactant alterations and alveolar epithelial apoptosis. We comparatively assessed the benefits of topical aSMase inhibition by either imipramine (Imi) or phosphatidylinositol-3,5-bisphosphate (PIP2) when administered into the airways together with surfactant (S) for fortification. In this translational study, a triple-hit acute lung injury model was used that entails repeated airway lavage, injurious ventilation and tracheal lipopolysaccharide instillation in newborn piglets subject to mechanical ventilation for 72 hrs. After randomization, we administered an air bolus (control), S, S+Imi, or S+PIP2. Only in the latter two groups we observed significantly improved oxygenation and ventilation, dynamic compliance and pulmonary oedema. S+Imi caused systemic aSMase suppression and ceramide reduction, whereas the S+PIP2 effect remained compartmentalized in the airways because of the molecule's bulky structure. The surfactant surface tensions improved by S+Imi and S+PIP2 interventions, but only to a minor extent by S alone. S+PIP2 inhibited the migration of monocyte-derived macrophages and granulocytes into airways by the reduction of CD14/CD18 expression on cell membranes and the expression of epidermal growth factors (amphiregulin and TGF-β1) and interleukin-6 as pro-fibrotic factors. Finally we observed reduced alveolar epithelial apoptosis, which was most apparent in S+PIP2 lungs. Exogenous surfactant "fortified" by PIP2, a naturally occurring surfactant component, improves lung function by topical suppression of aSMase, providing a potential treatment concept for neonates with hypoxemic respiratory failure.

Keywords: apoptosis • ceramide • macrophages • epithelial growth factors • fibrosis

Introduction

Hypoxemic respiratory failure of the neonate is a life-threatening manifestation of neonatal acute lung injury (nALI) that is defined as severely impaired lung function involving reduced lung compliance, permeability oedema, increased surfactant surface tension, transpulmonary migration of macrophages and alveolar epithelial apoptosis. A variety of clinical conditions ultimately cause nALI including (but not limited to) congenital pneumonia, sepsis, meconium aspiration and pulmonary haemorrhage, all of which are characterized by severe inflammation. An effective approach to pharmacological treatment remains to be elucidated. Severe hypoxemia may develop despite mechanical ventilation and surfactant replacement therapy, which results in an unacceptably high rate of mortality among the babies affected.

In nALI models, the physical properties of surfactant films are impaired by increased concentrations of the phospholipid ceramide [1, 2]. Ceramide is generated by the enzyme acid sphingomyelinase

*Correspondence to: Martin F. KRAUSE, M.D.
Department of Pediatrics, Universitätsklinikum Schleswig-Holstein, Campus Kiel, Schwanenweg 20, 24105 Kiel, Germany.
Tel.: +49-431-597-1622
Fax: +49-431-597-2771
E-mail: m.krause@pediatrics.uni-kiel.de

doi: 10.1111/j.1582-4934.2012.01618.x

(aSMase), which catalyses the degradation of cellular sphingomyelin to phosphorylcholine and ceramide. Ceramide inhibits the synthesis of dipalmitoyl- phosphatidylcholine (DPPC) by inhibiting the key enzyme cholinephosphate cytidylyltransferase [3]. The addition of ceramide to surfactant increases the surface tension of surfactant films in a dose-dependent manner [4]. Ceramide augments permeability oedema which further contributes to surfactant dysfunction [5]. Finally, ceramide mediates caspase-dependent [6] apoptosis, as evidenced in lung fibroblasts and airway epithelial cells [7].

L-α-phosphatidyl-D-myo-inositol-3,5-bisphosphate (PIP2) is a phosphoinositide that is important for stress signalling in organelles. PIP2 is rapidly derived from the ubiquitous surfactant component phosphatidylinositol by sequential phosphorylation by phosphoinositide kinases [8]. PIP2 is synthesized and excreted by type II pneumocytes in the lung [9], but it represents only a small portion of the total cell phosphoinositides (<0.1%). Most notably, PIP2 is the most potent aSMase inhibitor known to date, as demonstrated in cell culture studies [10, 11].

In a previous study we demonstrated the benefits of the non-specific aSMase inhibitor imipramine (Imi) for gas exchange, lung mechanics and pulmonary oedema in a nALI model of repeated airway lavage [2]. Because Imi has a high volume of distribution, its use in neonates may be perilous as a result of the systemic suppression of the critical aSMase-ceramide signal transduction pathway. Therefore, we evaluated topical PIP2 admixed with surfactant as an alternative because (i) it is produced naturally in the body, and (ii) it has a bulky molecular structure, which precludes distribution beyond the airway compartment.

In the present study, we used a neonatal porcine triple-hit lung injury model (repeated airway lavage, injurious ventilation and tracheal lipopolysaccharide instillation) throughout 72 hrs of mechanical ventilation. We focused on the comparison of the two test substances, Imi and PIP2 admixed with exogenous surfactant, and assessed the generalized non-specific Imi effect compared to the topical alveolar epithelial aSMase inhibition mediated by PIP2.

Materials and methods

The experimental protocol was approved by the review board of the Schleswig-Holstein government for the care of animal subjects (letter of acceptance V312-72241.121-24) in accordance with the German law for animal protection (BGBl 1, page 1319), and the European Community guidelines (2007/526/EC). A total of 30 piglets were studied between days 2 and 6 of life.

After sedation and intubation, mechanical ventilation was provided by pressure-limited neonatal ventilators with the following settings: FiO_2 = 0.5, PEEP = 6 mbar, and rate = 25/min. The peak (inspiratory pressure) was adjusted every hour to maintain the tidal volume (V_T) at 7 ml/kg. $PaCO_2$ was maintained within a range of 35–50 mmHg by controlling the rate and PaO_2 within 50–150 by controlling the FiO_2.

Repeated broncho-alveolar lavage (rBAL, first step of nALI) with 30 ml/kg saline was continued until the PaO_2/FiO_2 decreased to ~100 mmHg (baseline). At 25 hrs, the piglets were submitted to a 2 hrs-period of injurious ventilation (second step) with zero-PEEP ventilation followed by doubled V_T (14 ml/kg). In a third step, at 49 hrs, 2.5 mg lipopolysaccharide (*E. coli* serotype O127:B8) in 0.5 ml saline was instilled into the trachea.

The piglets were randomized to one of the following four groups:

- control (C) piglets received an air bolus;
- surfactant (S) piglets received 50 mg/kg surfactant (poractant alfa, Chiesi Farmaceutici, Parma, Italy);
- S+Imi piglets received 5 mg Imi admixed with surfactant;
- S+PIP2 piglets received 2 mg PIP2 (#10008398, Cayman, Tallinn, Estonia) admixed with surfactant.

Following each lung injury protocol the group-specific intervention was carried out three times (at 2, 26 and 50 hrs).

We calculated the oxygenation index [OI: MAP (mean airway pressure) × $\%O_2/PaO_2$] and a ventilation efficiency index [VEI: 3800/(Peak-PEEP) × f × $PaCO_2$]. Calculations of the extra-vascular lung water index (EVLWI, ml/kg) and cardiac index (CI, l/min./m^2) were performed using the transpulmonary indicator dilution technique [2]. The single-breath least square method was used to assess the dynamic (specific) compliance (sC_{rs}) and resistance (R_{rs}) of the respiratory system as previously described [12].

Prior to killing the piglets a final diagnostic BAL (dBAL) was carried out; lung tissue specimens were then gathered for the subsequent analyses.

BALF cell counts and differentials: BALF was filtered to remove gross particles and secretions from the airways, and was centrifuged for 4 min. at 4°C and 20 × *g* to separate cells. Cellular material was resuspended into phosphate-buffered saline for cell counts, cell differentiation by standard Romanowsky staining, and for flow cytometry. For flow cytometry the cell pellet was resuspended in 30 μl blocking reagent and 120 μl washing buffer. After a washing step, surface staining with a combination of FITC- (CD14 antigen, IgG2a) and PE- (CD18 antigen, IgG1) conjugated monoclonal antibodies and their appropriate isotype controls (all reagents from antibodies-online, Aachen, Germany) was achieved by incubation of ~10^5 cells with the monoclonal antibody cocktails for 30 min. at 4°C in the dark. Cells were subsequently analysed using flow cytometry using a FACSCalibur and the CellQuest software (Becton Dickinson, Heidelberg, Germany).

Surfactant was isolated by filtering and centrifuging BALF for 5 min. at 4°C and 20 × *g*. The pellet was then weighed and resuspended in normal saline at a concentration of 10 mg/ml thus assessing surfactant quality only and disregarding the individual surfactant pool in the piglets. Surfactant in aliquots of 0.5 ml was put on the surface of a warmed normal saline trough for determination of minimal (and maximal) surface tension by the use of a modified Wilhelmy balance (E. Biegler, Mauerbach, Austria).

Real-time qPCR for the quantification of amphiregulin, TGF-β1, IL-6: RNA isolation was performed with 30 mg lung powder with NucleoSpin RNA II Kit (Machery Nagel, Düren, Germany) automated on QIAcube roboter (Qiagen, Hilden, Germany). RNA quantification and quality control was done using a NanoDrop 1000 spectrophotometer (Thermo Fisher, Waltham, MA, USA). 675 ng of RNA, 1 μl oligo$(dT)_{15}$ primer (0.5 μg/μl; Invitrogen, Karlsruhe, Germany) were added in a total volume of 12 μl of H_2O. After 10 min. incubation at 65°C on a UNO II thermocycler (Biometra, Göttingen, Germany), five times 4 μl buffer, 2 μl dNTP (10 mM), 1 μl RNasin (40 U/μl), and 1 μl M-MLV RT [13] (200 U/μl; all reagents from Promega, Mannheim, Germany) were added. This was followed by two incubation periods of 90 min. at 40°C, and 5 min. at 95°C, respectively, on UNO II thermocycler. Real-time qPCR: 1 μl cDNA as template was incubated with 312.5 nM forward

primer (248 nM for Il-6; Eurofins, Ebersberg, Germany), 312.5 nM reverse primer (248 nM for Il-6) and SYBR-Green I Mastermix (Roche Diagnostics, Mannheim, Germany) in a LightCycler480 (Roche). Cp values were acquired by the Second Derivative Maximum method. Advanced relative quantification was performed using the LightCycler 480 Software 1.5 SP3 (Roche), and efficiency corrected by in-run standard curves using the Roche Applied Science E-Method [14]. Data were referenced to the correspondent housekeeping gene ß2-microglobulin and normalized to the mean of the C-group values. For quality control, in-run negative controls, melting curve profiles and product separation in agarose gels were performed.

aSMase activity and ceramide concentrations in pulmonary tissues, BALF and serum: aSMase activity were assayed in a modified micellar *in vitro* assay using sphingomyelin labelled with carbon 14 (^{14}C) (Amersham Pharmacia Biotech, Piscataway, NJ, USA) as substrate, as described by Wiegmann *et al.* [15]. Frozen lung tissue samples were pulverized and melted, of which 10 μg of protein was used to assay aSMase activity in the presence of 1.4 mM $ZnCl_2$ in a buffer (final volume of 50 μl) containing 250 mM sodium acetate, 1 mM EDTA (pH 5.0) and 2.25 μl of [N-methyl-^{14}C]sphingomyelin. $Zn2^+$ dependency was assayed by replacing $Zn2^+$ by 1 mM EDTA. Phosphorylcholine was then extracted with 800 μl of chloroform/methanol (2:1 [vol/vol]) and 250 μl of H_2O and the amount of radioactive phosphorylcholine produced from hydrolysis of ^{14}C-sphingomyelin determined in the aqueous phase by scintillation counting. For aSMase activity measurements in fluids (BALF and serum), initially 30 μl fluid were mixed with 280 μl aSMase-buffer, and identical steps were taken for final scintillation counting.

Ceramide levels were determined as described by Jensen *et al.* [16] after extraction from homogenized tissue by chloroform/methanol, separation of lipids by high performance thin-layer chromatography, and quantification by two-dimensional charring densitometry.

TUNEL staining for the quantification of alveolar epithelial apoptosis: *In situ*-tailing was applied to visualize DNA fragmentation in apoptotic cells (#11684817910, Roche Applied Science). Sections were deparaffinized, rehydrated, boiled in citrate buffer and immersed in TritonX-100/hydrogen peroxidase. Non-specific staining was reduced by incubating sections with 3% bovine serum albumin/Tris buffered saline for 1 hr in room temperature before applying the TUNEL reaction mixture (1 hr, 37°C in humidified chambers). After washing, converter-peroxidase was incubated on the slides for 30 min. at 37°C. Labelling was visualized by adding DAB substrate (Roche) for 10 min. Negative controls were performed by omitting the TUNEL reaction mixture during the labelling step, which resulted in absence of specific staining. Apoptosis was assessed by light microscopy using an alveolar epithelial apoptosis score: 4–6 alveoli per section were chosen to determine the number of apoptotic cells in an undisturbed alveolar epithelial lining of 200 cells as a reference. The colleague performing the score (SP) was blinded to the sections' group affiliation.

Immunohistochemical detection of (active) caspase-8 [17]: Paraffin-embedded lung specimens were sectioned at 1 μm. Before staining sections were deparaffinized, rehydrated, washed in Tris buffered saline and boiled in fresh citrate buffer (pH 6) using microwave for 10 min. Endogenous peroxidase activity was blocked, and sections were permeabilized by incubation in 0.3% TritonX-100/1% hydrogen peroxidase for 20 min. Sections were then blocked with 10% donkey serum (Dinova, Hamburg, Germany) for 1 hr at room temperature, and the antibody against (active) caspase-8 (rabbit-IgG; Cell Signalling, New England Biolabs, Frankfurt, Germany) was incubated at 4°C overnight. Signals were amplified using the avidin-biotin-complex method (Vectastain peroxidase kit, Vector Laboratories, Burlingame, CA, USA) and visualized with diaminobenzidine. Finally, sections were counterstained with Hämalaun (Sigma, München, Germany), dehydrated in an ascending row of ethanols before mounting with Eukitt (Kindler, Freiburg, Germany), and cover-slipped for assessment using light microscopy.

Non-parametric data (cell differentials, growth factors, cytokines and apoptosis score) were checked for heteroscedasticity and, when necessary, corrected using the Box-Cox transformation before analysis. The differences between groups were analysed by an univariate ANOVA followed by Dunnett's post-test only when the omnibus test showed significant treatment effects. For single-group comparisons, we used two-tailed unpaired *t*-tests. A repeated measures two-factorial ANOVA for the clinical parameters (Figs 2 and 3), with time and treatment ("treat") as independent variables, was used to highlight the intermediate-term effects of the specific interventions at the following times: 12–24, 36–48 and 60–72 hrs.

All data represent the means ± SEM unless otherwise specified. $P < 0.05$ was considered to be significant. All analyses were performed using GraphPad Prism 5 and JMP 9.0.

Supplementary information on Materials and Methods is available at the journal's website at http://www.blackwellpublishing.com/journal.asp?ref=1582-1838.

Results

An outline of the experimental protocol is provided in Figure 1.

Two piglets in the S+Imi group did not complete the entire study period and were excluded from the data analysis. Both were diagnosed with acute renal failure (creatinine 152 μmol/l, potassium >10 mmol/l at 52 hrs; oliguria and potassium >9 mmol/l at 42 hrs).

To establish comparability of the four groups at the start of the study ("intact lung"), we confirmed that age, weight, initial PaO_2/FiO_2 and Peak (inspiratory pressure), as well as the number of lavages needed to achieve a PaO_2/FiO_2 ~100 mmHg and a Peak $\geq$ 19 m bar, and the loss of lavage fluid in the airways were similar (Table 1).

Clinical parameters

The clinical parameters OI, VEI, sC_{rs} and EVLWI (Figs 2 and 3) were compared by selecting three time intervals (12–24, 36–48 and 60–72 hrs), which were chosen to assess the intermediate-term (not short-term effects) effects of the interventions. A summary of treatment effects is provided in Table 2 and proves the superiority of S+PIP2 treatment for all four parameters when compared to S alone. EVLWI effects are not apparent before 60–72 hrs. sC_{rs} and EVLWI are equally influenced by S+Imi and S+PIP2. To assess alveolar stability, the "25 hrs" time point after completion of the 1 hr interval of zero-PEEP ventilation (first part of the second protocol of nALI, injurious ventilation) was compared among groups, and the "72 hrs" time point at study end was evaluated similarly, reflecting all lung injury protocols and all interventions to some extent. Significant differences between the groups were found for OI (25 hrs $P < 0.01$, 72 hrs $P < 0.001$; univariate ANOVA), VEI

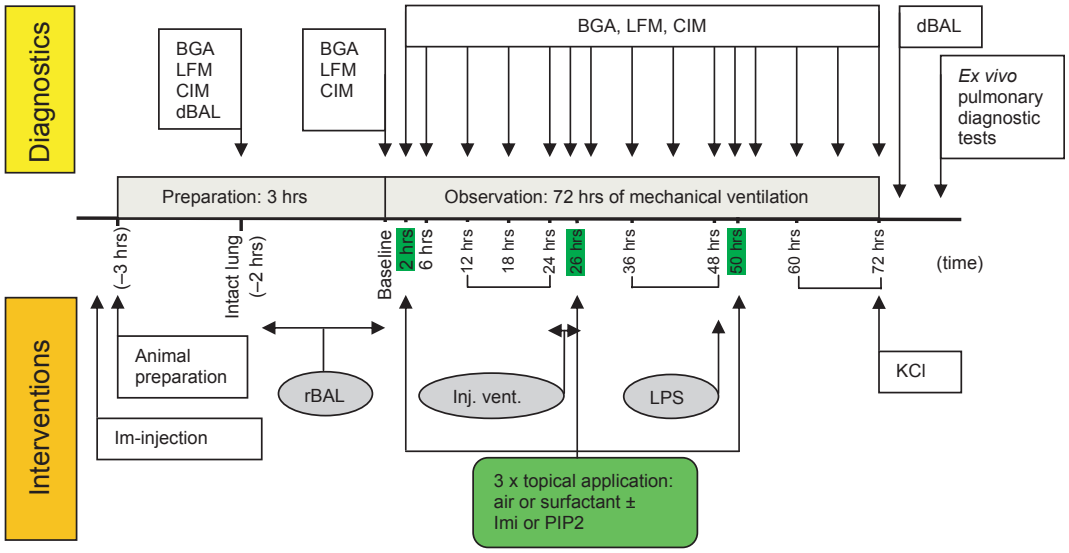

Fig. 1 Flow chart of the experimental protocol covering an observational time interval of ~75 hrs [consisting of 3 hrs of preparation and 72 hrs of mechanical ventilation (beige)]. Diagnostics (yellow) in the upper half: BGA, blood gas analysis; LFM, lung function measurement; CIM, cardiac index monitoring; dBAL, diagnostic bronchoalveolar lavage. Interventions (orange) in the lower half: Triple-hit lung injury is indicated in grey boxes consisting of rBAL, repeated bronchoalveolar lavage; inj. vent., injurious ventilation; and LPS, tracheal instillation of lipopolysaccharide. Topical application of surfactant preparations (or air in the control-group, green) at 2, 26 and 50 hrs. KCl, intravenous injection of potassium chloride at study end. The brackets indicate the time intervals selected for statistical evaluation of the clinical parameters which were chosen to highlight the intermediate-term (not short-term effects) effects of surfactant ± aSMase inhibitor application.

Table 1 Group comparisons before repeated airway lavage ("intact lung")

	C (n = 6)	S (n = 6)	S+Imi (n = 8)	S+PIP2 (n = 8)	P
Age (d)	4.3 ± 0.7	3.8 ± 1.5	4.2 ± 0.4	3.7 ± 0.8	0.35
Weight (kg)	2.5 ± 0.4	2.8 ± 0.2	2.6 ± 0.1	2.4 ± 0.4	0.35
Female (n)	2	2	3	1	–
PaO_2/FiO_2 (mmHg)	331 ± 88	422 ± 72	397 ± 75	359 ± 75	0.20
Peak (mbar)	13.2 ± 1.9	12.6 ± 2.0	13.7 ± 2.1	11.8 ± 1.9	0.32
Lavages (n)	13.5 ± 2.7	16.0 ± 3.2	16.6 ± 3.4	17.0 ± 4.6	0.31
Loss of lavage fluid (%)	10.2 ± 2.6	9.6 ± 3.3	9.2 ± 2.5	9.5 ± 2.9	0.91

Peak = peak inspiratory pressure. Data represent the means ± SD. Univariate ANOVA.

(25 hrs $P < 0.05$), sC_{rs} (72 hrs $P < 0.001$) and EVLWI (72 hrs $P < 0.05$).

Surfactant surface tensions

Minimum surface tensions of surfactant from BALF varied significantly (Fig. 4). To demonstrate the ability of our system to lower surfactant surface tension (a Wilhelmy balance) we confirmed that the addition of 5 mg poractant alfa onto the surface of the saline bath yielded a minimum tension of 19.0 ± 0.1 mN/m, and the addition of 10 mg a tension of 5.9 ± 0.8 mN/m.

Cell concentrations, differentials and cell subsets in BALF

The total cell count in BALF varied significantly between groups after 72 hrs of mechanical ventilation (Fig. 5A). The average pre-lavage cell concentration was approximated by the intervention with S+PIP2

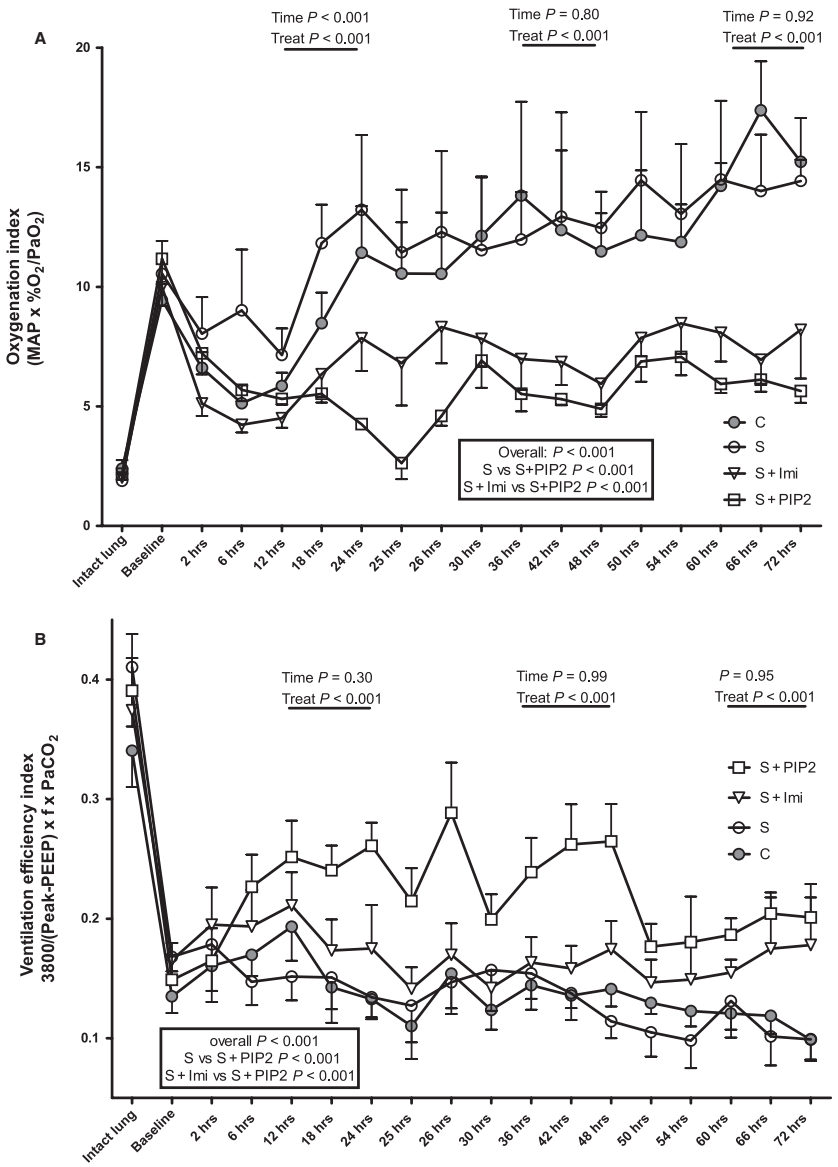

Fig. 2 Oxygenation index (**A**), and ventilation efficiency index (**B**), according to the experimental protocol as outlined in Figure 1. MAP, mean airway pressure; Peak, peak inspiratory pressure; PEEP, positive end-expiratory pressure. Data represent the means ± SEM, repeated measures two-factorial [time and treat(ment)] ANOVA. Significant treat(ment) effects could be calculated for oxygenation index and ventilation efficiency index for all three time intervals, as well as for a combination of these three time intervals (text box results) comparing both all four groups ("overall") and selected pairs of groups. Interactions of the two independent factors "time" and "treat(ment)" were not significant.

only ($130 \pm 42 \times 10^3$ cells/μl *versus* $149 \pm 46 \times 10^3$). The BALF cell differentials showed decreased percentages of granulocytes and increased percentages of monocytes after aSMase inhibition, an effect that was only significant for S+PIP2 treatment (Fig. 5B).

Lung injury induced a two- to fivefold increase in $CD14^+$ and/or $CD18^+$ cells (Fig. 5C, C group). Notably, S+Imi and S+PIP2 significantly reduced the number of $CD14^+/18^+$ cells, whereas $CD14^-/CD18^+$ cells were only reduced by S+PIP2 intervention ($P < 0.01$).

Amphiregulin, TGF-β1, and IL-6

Surfactant alone (S) produced equal or slightly increased gene expression compared to that observed in the C group, and only S+PIP2 significantly decreased gene expression to a remarkably low level (Fig. 6).

aSMase activity and ceramide

Compared to the C group, S+Imi reduced aSMase activity in pulmonary tissues by 41.9% (Fig. 7A). There was a 33.2% reduction in the levels of ceramide (Fig. 7B). Because the reduction in aSMase activity in S+PIP2 treated lungs was similar to the S-treated lungs, and no additional effect on aSMase inhibition could be detected, we also compared aSMase activities in the alveolar (Fig. 7C) and blood (Fig. 7D) compartments. The results show that 1. the local alveolar inhibition was even more pronounced

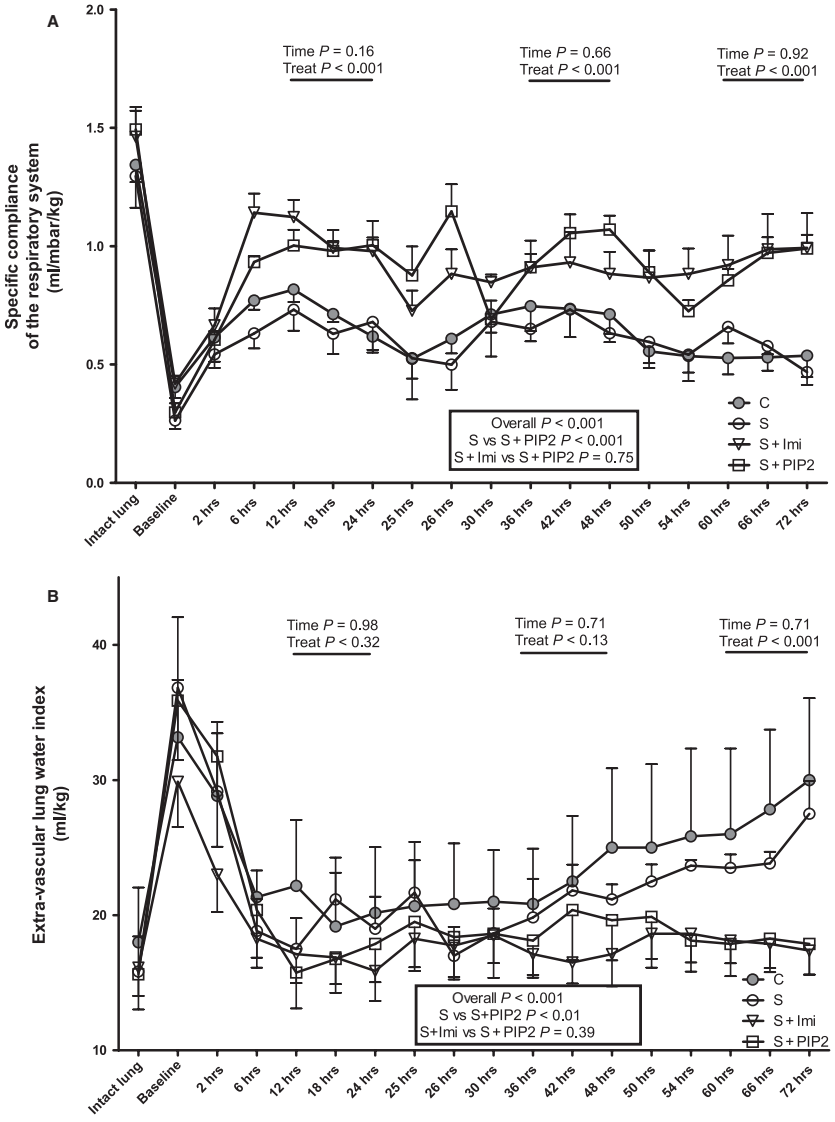

Fig. 3 Specific compliance of the respiratory system (**A**), and extra-vascular lung water index (**B**) according to the experimental protocol as outlined in Figure 1. Data represent the means ± SEM, repeated measures two-factorial [time and treat(ment)] ANOVA. Significant treat(ment) effects could be calculated for compliance at all three time intervals, for extra-vascular lung water index at the 60–72 hrs interval, as well as for a combination of these three time intervals (text box results) comparing both all four groups ("overall") and S *versus* S+PIP2. Interactions of the two independent factors "time" and "treat(ment)" were not significant.

(but not significantly different) after treatment with S+PIP2 compared to S+Imi, and 2. only S+Imi, but not S+PIP2, exerted a systemic effect by balancing the aSMase activity levels in serum over time.

TUNEL staining, apoptosis score, and caspase-8 immunohistochemistry

Assessment of alveolar epithelial apoptosis revealed a significant reduction in S+PIP2 treatment compared to S treatment alone (Fig. 8A). Graphic representatives of cells with alveolar apoptosis by TUNEL staining (Fig. 8B) and immunohistochemical staining of active caspase-8 (Fig. 8C) are provided by means of an enlargement.

Intervention-related side effects

To investigate any relevant side effects, we also monitored the resistance of the respiratory system, cardiac index and systemic vascular resistance index, fluid and electrolyte balances, hepatic and renal serum parameters and differential blood cell counts over 72 hrs of mechanical ventilation (data not given). Differences between the groups were only observed for urine production (C: 5.8 ± 0.6 ml/kg/h, S 4.4 ± 0.8, S+Imi 4.6 ± 0.4, S+PIP2 3.8 ± 0.4; $P = 0.07$,

Table 2 Summary of treatment effects on clinical parameters

Time interval	12–24 hrs	36–48 hrs	60–72 hrs	Overall	S *versus* S+PIP2	S+Imi *versus* S+PIP2
OI	<0.001	<0.001	<0.001	<0.001	<0.001	<0.001
VEI	<0.001	<0.001	<0.001	<0.001	<0.001	<0.001
sC_{rs}	<0.001	<0.001	<0.001	<0.001	<0.001	0.75
EVLWI	0.32	0.13	<0.001	<0.001	<0.01	0.39

P-values of treatment effects ("treat" in Figs 2 and 3) for the four clinical parameters comparing all four groups by repeated measures two-factorial ANOVA. "Overall" indicates the combination of the three intervals 12–24, 36–48 and 60–72 hrs. Single group comparisons (S *versus* S+PIP2 and S+Imi *versus* S+PIP2) of all three intervals. The second factor "time" as well as interactions of "treat" and "time" were not significant for either parameter.

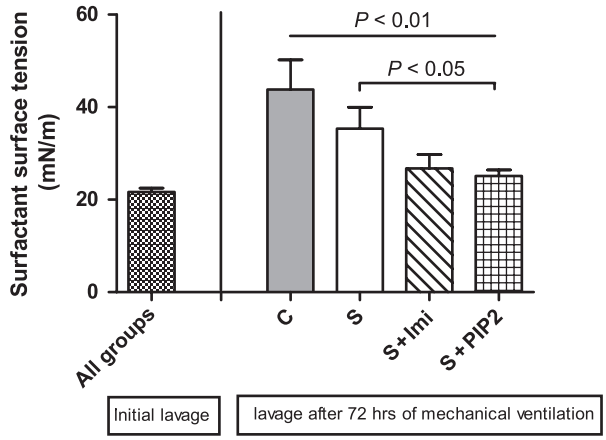

Fig. 4 Surfactant surface tension of the surfactant films from the initial bronchoalveolar lavage (all groups) and the lavage after 72 hrs of mechanical ventilation. A total of 5 mg of surfactant were given on the saline surface of a modified Wilhelmy balance; measurements were taken at the minimum surface (12.8 cm^2). Data represent the means ± SEM. Univariate ANOVA, Dunnett's post-test. Overall comparison $P < 0.01$, S *versus* S+PIP2 $P < 0.05$.

univariate ANOVA) and weight gain (C: +0.34 ± 0.02 kg/kg/72 hrs, S + 0.32 ± 0.03, S+Imi + 0.36 ± 0.03, S+PIP2 + 0.47 ± 0.03; $P < 0.05$).

Discussion

The four clinical parameters oxygenation (OI) and ventilation (VEI), compliance (sC_{rs}) and pulmonary oedema (EVLWI) (Figs 2 and 3) improved significantly after topical airway epithelial aSMase inhibition when compared to the C and the S groups. Because the beneficial surfactant effects subside more than 6–12 hrs after replacement therapy in inflammatory lung disease (as also demonstrated in the present study), the benefits of clinical application in term neonates [18], in children [19] and especially in adult patients [20] suffering from ALI/ARDS are not convincing. Additional treatment strategies will be necessary to restore epithelial and endothelial functional integrity.

PIP2: aSMase inhibition and metabolism

Lipid rafts on the membranes of pulmonary epithelial and endothelial cells are constituted of cholesterol and sphingolipids (sphingomyelin and glycolipids) and are located in the exoplasmic leaflet of the plasma membrane [21]. These rafts have a diameter of ~50 nm, corresponding to ~3500 sphingomyelin molecules and a limited set of structural proteins (~10–30) [21, 22]. Thus, >75% of cellular sphingomyelin is concentrated in the rafts [23]. They also contain the enzyme aSMase (effector, Fig. 9), which is subject to rapid activation following stress and produces ceramide from sphingomyelin. Developmental changes increase the levels of aSMase activity and ceramide content in the foetal and neonatal lung when compared to the adult lung as evidenced in rats [24].

Ceramide and its downstream products sphingosine and sphingosine-1-phosphate are recognized as second messengers and ultimately regulate cell growth, viability, differentiation and senescence [22]. Ceramide, a phospholipid, has been proven to increase surfactant surface tension by integration into the surfactant film [4], to induce permeability oedema by epithelial/endothelial disruption [5], and to cause apoptosis [7]. As a consequence, pharmacological inhibition of increased aSMase activity by non-specific aSMase-inhibitors such as Imi improved pulmonary functions in selectively perfused murine lungs [5] and in a neonatal piglet model of respiratory failure [2]. Because Imi exerts a broad range of undesired effects mediated by the induction of lysosomal proteases and has a high volume of distribution (14.5 l/kg), we comparatively assessed the effects of PIP2, a naturally occurring specific aSMase inhibitor without cell membrane penetrating properties.

PIP2 has been shown to suppress aSMase activity by 47% in cell cultures and is regarded as the most potent (IC_{50} = 0.53 μmol = 0.51 mg/ml) selective aSMase inhibitor known to date [10]. Recent research revealed that PIP2 is less suitable for cell culture research because of its fivefold negative charge and its two long fatty acid chains (16:0/16:0), which cause it to stack in cellular membranes [11]. For clinical use in sick neonates, however, limited tissue penetration and organ translocation of PIP2 are rather desirable for protecting the delicate neonatal organism [25, 26] from systemic immune suppression. To demonstrate a local (compartmentalized) PIP2 effect within the airspaces, we detected lower aSMase activity in

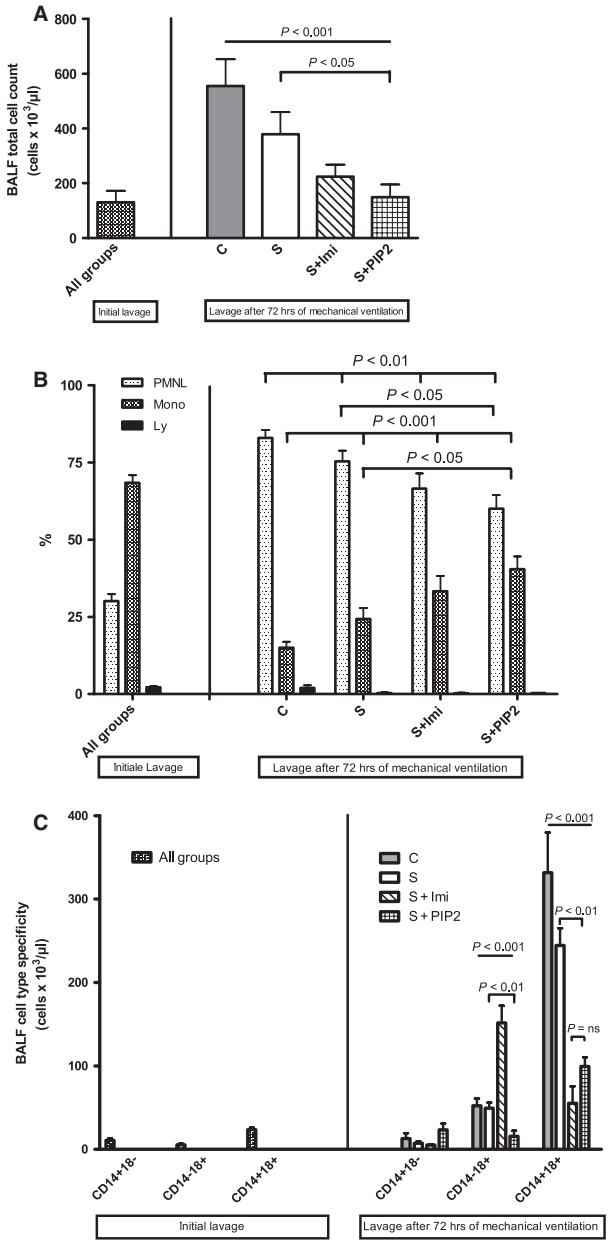

Fig. 5 (**A**) BALF total cell count from the initial lavage (all groups) and from the lavage after 72 hrs of mechanical ventilation. (**B**) BALF cell differentials by light microscopy. (**C**) BALF cell type specificity identifying $CD14^+$ and $CD18^+$ cells. Data represent the means ± SEM. Univariate ANOVA, Dunnett's post-test (S *versus* S+PIP2). BALF, bronchoalveolar lavage fluid; PMNL, granulocytes (polymorpho-nuclear leukocytes); Mono, monocytes; Ly, lymphocytes.

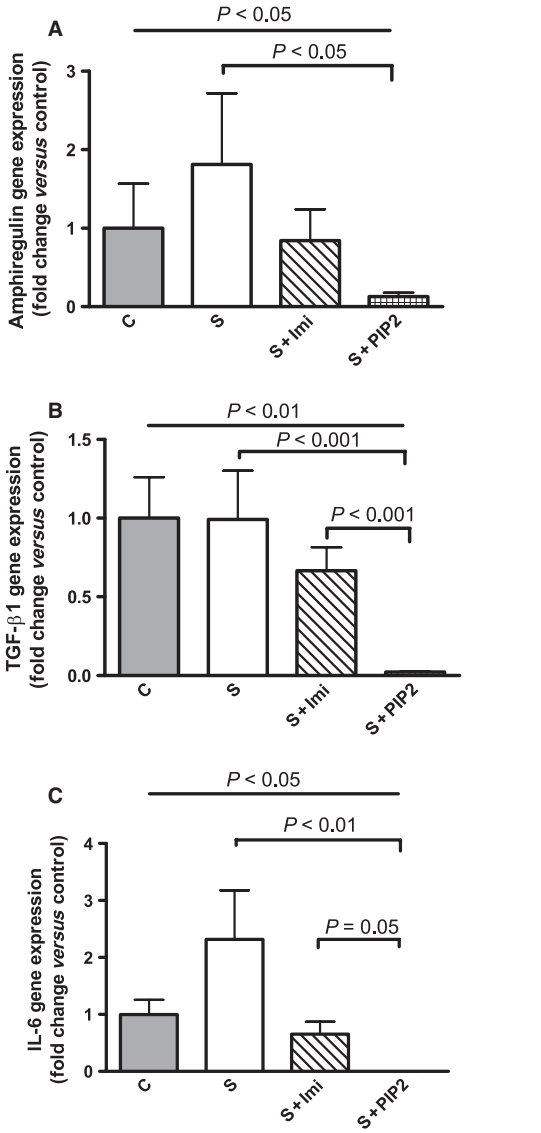

Fig. 6 Amphiregulin (**A**), transforming growth factor-β1 (TGF- β1) (**B**), and interleukin-6 (IL-6) (**C**) gene expression in pulmonary tissues as determined by real-time quantitative polymerase chain reaction, after 72 hrs of mechanical ventilation. Efficiency corrected values were referenced to the housekeeping gene ß2-microblobulin and then normalized to the mean of the C-group values. Data represent the means ± SEM. Univariate ANOVA, Dunnett's post-test.

the BALF in the S+PIP2 condition compared to S+Imi-treated piglets (Fig. 7C). As extracellular aSMase activity is present in all body fluids except cerebrospinal fluid [27], the systemic aSMase inhibiting effect found in S+Imi piglets confirms an unrestricted Imi distribution (Fig. 7D). However, given the extracellular location of aSMase in the outer leaflet of the plasma membrane, an inhibitor does not need to be cell permeable [5].

Phosphorylation of the phosphatidyl-inositol (PtdIns) head group generates eight varieties of phosphoinositides including PtdIns-3-P, PtdIns-4,5-P2 and PtdIns-3,5-P2 (PIP2). PtdIns-3-P serves as a precursor for PIP2, the latter only reaching concentrations that are ~500-fold lower [28]. PtdIns increases by fourfold in the BALF of adult

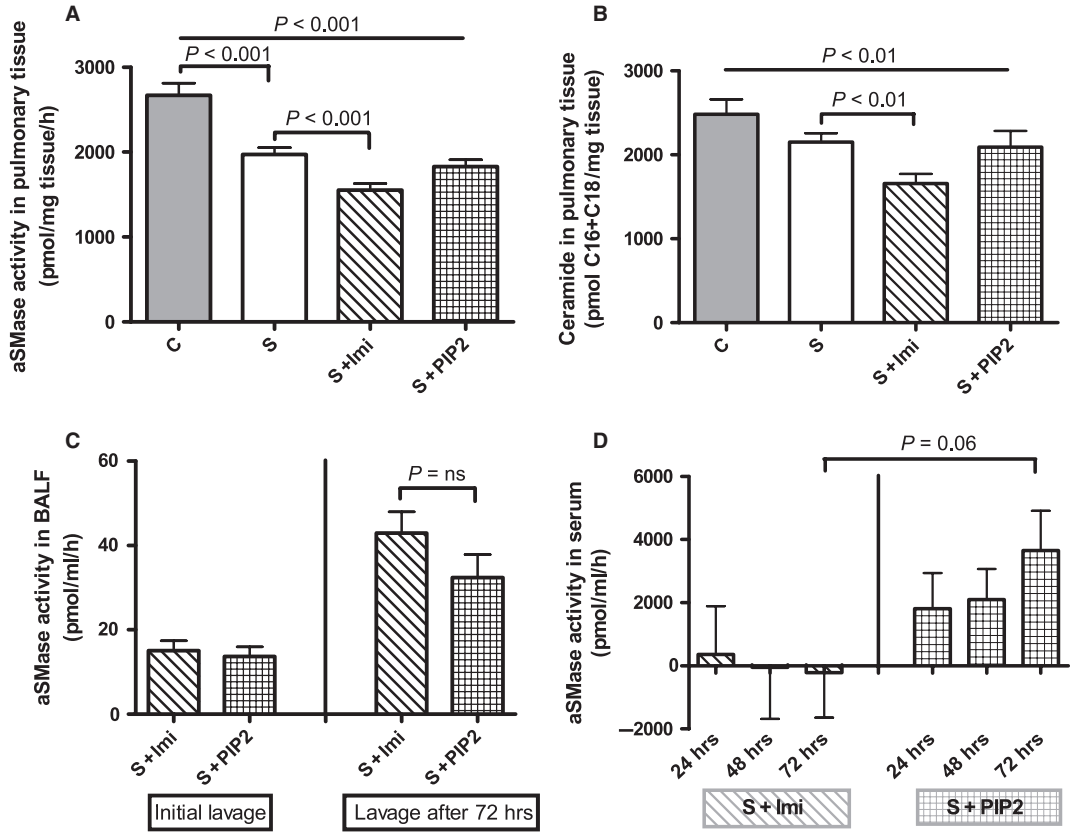

Fig. 7 aSMase activity (**A**) and ceramide concentrations in pulmonary tissues (**B**) after 72 hrs of mechanical ventilation; aSMase activity in the BALF (**C**) from the initial lavage and after 72 hrs, S+Imi and S+PIP2 groups only, aSMase activity in serum over time (**D**), S+Imi and S+PIP2 groups only. Data represent the means ± SEM, univariate ANOVA followed by Dunnett's post-tests in **A**+**B**, unpaired *t*-tests in **C**+**D**.

ARDS patients as a result of decreased levels of PtdIns-specific extracellular phospholipase C activity [29]. Whether or not this increase in PtdIns also serves to counteract pulmonary inflammation and increase the percentage in 16:0/16:0-PtdIns (usually only ~3% of PtdIns in human surfactant), the basic compound for PIP2 synthesis, is not known to date. *Saccharomyces* cells exposed to hyperosmotic medium increase their PIP2-levels 20-fold within 5 min. [30] and return to normal 20 min. later. The sustained effects of the S+PIP2 emulsion in the present study suggest, however, decelerated PIP2 release and metabolism from the surfactant emulsion when compared to the aqueous solutions used for cell culture research.

Effector modulations

Alveolar epithelial apoptosis

Hyaline membranes, protein-rich alveolar exudates, fibroproliferative changes and epithelial apoptosis all contribute to the impaired gas exchange and lung functions in nALI (Fig. 9). Relative to apoptosis, Bern *et al.* [31] demonstrated 1–20% caspase-3 positive pre-apoptotic epithelial cells in pulmonary specimens from children who died of hypoxemic respiratory failure. Aside from developmental processes, lung epithelial apoptosis in newborns and infants occurs in conditions such as respiratory tract infection (including LPS-induced nALI), meconium aspiration, exposure to high oxygen concentrations and mechanical stress [32]. Overt apoptosis is observed only in a minority of alveolar epithelial cells in nALI, but gas exchange is impaired in many more cells as a result of dysfunction of membrane pumps, dissolution of tight junctions and reduced ATP levels [33]. Epithelial apoptosis is mediated by mechanical stretch imposed on type II pneumocytes [34], LPS [35], and cross-talk between ceramide and the caspases [36]. According to the "neutrophilic hypothesis" [37], epithelial apoptosis depends on granulocyte apoptosis, clearance of apoptotic granulocytes in airspaces and their phagocytosis by macrophages leading to phenotype change and decreased production of pro-inflammatory mediators. We suggest, however, that the low aSMase concentrations found in the BALF of S+PIP2-treated piglets (Fig. 7C) essentially inhibited migration of granulocytes and monocyte-derived macrophages into the airspaces [38], suppressed their metabolic activity [39] and modulated the epithelial inflammatory response [36, 40] ("epithelial hypothesis").

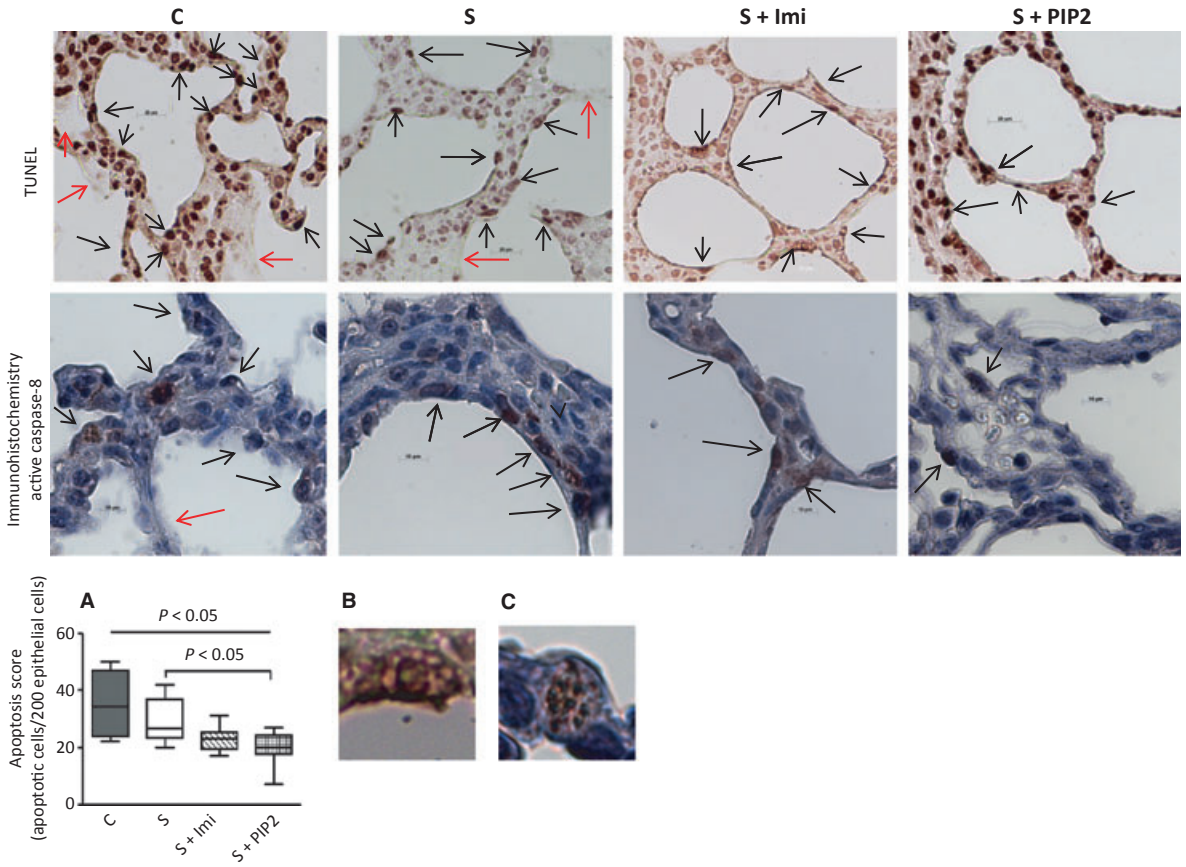

Fig. 8 First row: Terminal deoxynucleotidyl transferase dUTP nick end labelling (TUNEL) of representative sections from pulmonary tissues. Scale bar = 20 μm, oil × 800. Black arrows indicate apoptotic alveolar epithelial cells, red arrows indicate hyaline membranes. To minimize background fluorescescence BSA concentration was increased to 3% in the TdT staining buffer. Second row: Active caspase-8 staining by immunohistochemistry in the alveolar epithelium. Scale bar = 10 μm, oil × 1200. Black arrows indicate caspase-8-positive alveolar epithelial cells, the red arrow indicates a hyaline membrane. The antibody against caspase-8 was omitted for negative controls. Apoptosis score (**A**) representing the number of apoptotic epithelial alveolar cells out of 200 cells from an alveolar epithelial syncytium of a minimum of three and a maximum of six alveoli. The boxes extend from the 10th to the 90th percentile, and the whiskers describe the extremes. Univariate analysis of variance, Dunnett's post-test (S *versus* S+PIP2). Graphic representatives of single cells stained by either TUNEL (**B**) or by immunohistochemistry (**C**).

Transpulmonary cell migration

Migration of the $CD14^+/CD18^+$ cell subset (essentially monocyte-derived macrophages and granulocytes) was inhibited by S+Imi and by S+PIP2 treatment. Maus *et al.* showed in a murine model of MCP1-induced ALI that blood monocytes and resident alveolar macrophages, in contrast to monocyte-derived macrophages, do not express CD14 [41]. Because CD14/LPS-interactions result in cellular signalling and production of pro-inflammatory cytokines, reduced CD14 expression may be an important effector modulation to reduce uncontrolled pulmonary inflammation [42].

In contrast, CD18 is expressed on all three monocyte-derived cell lines as well as on granulocytes. In LPS-induced lung injury in rabbits, blockade of the adhesion receptor CD18 (β2-integrin) with a monoclonal antibody resulted in reduced granulocyte invasion and permeability edema but did not influence macrophage recruitment [43]. S+PIP2 treatment exerted significant reductions in CD14 *and* CD18 expressions: the former is an effect of Imi that has been previously described in cell cultures stimulated by LPS or ceramide [44], the latter represents a new finding, which contributed to the reduced percentages of granulocytes and the reduced cell concentrations in BALF.

Growth factors and IL-6

Amphiregulin is a polypeptide epithelial growth factor receptor (EGFR) ligand in airway epithelial cells, and its expression follows exposure to stressors such as stretch-mediated overventilation [45, 46]. This effect was significantly suppressed by S+PIP2 intervention in our model (Fig. 6A), which also involved a 60-min period of overventilation (at

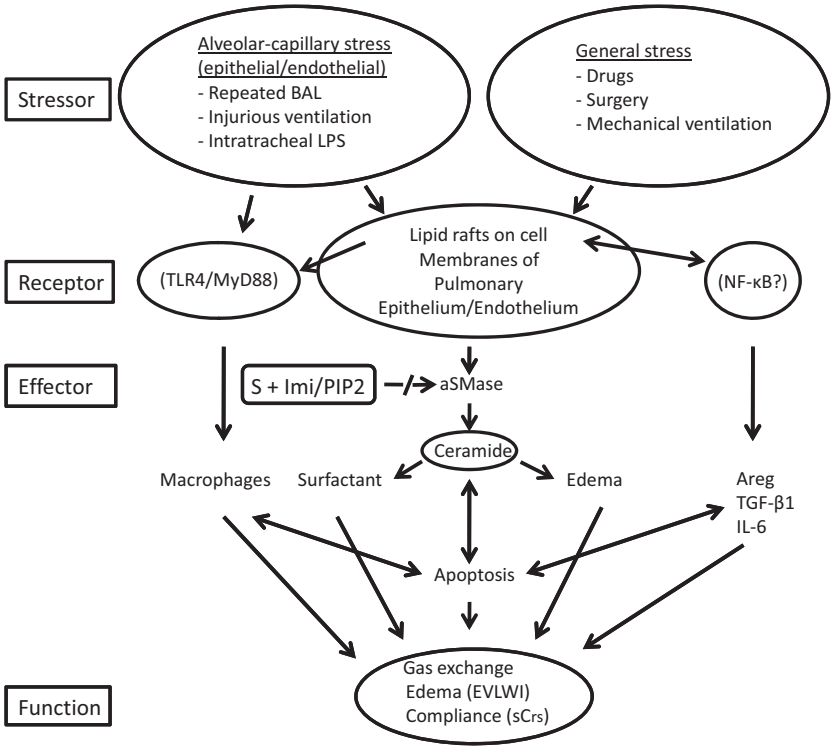

Fig. 9 Theoretical structure of this triple-hit nALI model as a translational study. There are specific stressors to the alveolar epithelial/endothelial cells (first bubble) and general stressors (second bubble) because of the set-up of the model. The study contains three levels of assessment: receptor, effector, and (lung) function. Toll-like receptor 4 (TLR4), myeloid differentiation primary response gene 88 (MyD88), and nuclear factor-κB (NF-κB) were not assessed in this study but are known to play important roles for migration of macrophages into airways, and transcription of genes for amphiregulin, TGF-β1, and IL-6 synthesis, respectively. The aSMase/ceramide pathway is displayed as the central pro-inflammatory pathway causing impaired lung function as assessed by oxygenation, ventilation, compliance and pulmonary edema. Topical application of S+Imi/PIP2 for suppression of aSMase activity and improved lung function.

26 hrs). TGF-β1 (Fig. 6B), a pleiotropic polypeptide involved in both the positive and negative regulation of cell proliferation and differentiation [47], is recognized as a driving force in fibroproliferation in the acute/subacute phases of ALI/ARDS [48, 49], and its expression is mutually dependent on ceramide generation [47]. The marked reductions in TGF-β1 and amphiregulin mediated by S+PIP2 are novel effects that might improve the prognosis of nALI in human neonates as a result of the protection against fibroproliferative lung repair. Whether suppression of TGF-β1 expression occurred because of the aSMase suppression or by direct PIP2-interactions cannot be deduced from the data of this study. Pekary & Hershman [50], however, suggested different second messenger signalling pathways for TNF-α-induced aSMase activation and TGF-β1 activation by MAP kinases and the MAD protein pathways, an observation rather favouring a direct PIP2-effect. The marked reduction in IL-6 as a cytokine with universal impact in pulmonary inflammation, atelectasis/alveolar recruitment [51] and cyclic stretching of endothelial cells [52], observed in S+PIP2-treated piglets could also contribute to the reduced stimulation of alveolar epithelial cells and macrophages producing collagen fibres [53].

Surfactant function and pulmonary oedema

Surfactant function (Fig. 4) and pulmonary oedema (Fig. 3B) differed significantly between groups. Although the effect of ceramide on surfactant function is twofold, direct as a result of the integration into the surfactant film [4], and indirect, *e.g.* because of the decreased surfactant protein B gene expression [54], the mechanisms behind oedema generation are less obvious. In all likelihood alterations of the endothelial cells with increased permeability are followed by activation of ceramide-binding proteins and can be inhibited by several serine/threonine protein kinase inhibitors [55].

Triple-hit neonatal acute lung injury (nALI)

Presuming that the aSMase/ceramide pathway is a central pro-inflammatory pathway in nALI models [5, 56], our intention was to maximize the clinical relevance of our translational model through the application of different local stressors to the pulmonary epithelium/endothelium, each of which is able to induce respiratory failure by itself in piglet nALI models: repeated airway lavage, injurious ventilation and tracheal LPS instillation (Fig. 9, stressors). A more detailed discussion of this model is provided in a previous publication [57].

Limitations of this study

PIP2 dosage: We used 2 mg PIP2 dissolved in 2.5 ml/kg (~0.32 mg/ml) poractant alfa given into an estimated functional residual capacity of ~20 ml/kg after repeated airway lavage. Mindful of bronchoalveolar lining fluid and extra-alveolar pulmonary oedema, the final concentration of PIP2 may be lower. The only PIP2 dosage for cell culture studies was provided by Kölzer *et al.* [10] using concentrations of 0.51 mg/ml to achieve aSMase inhibition of 47%, which is comparable to the reduction in the present study. In a neonatal piglet

lavage model [2], we showed that S+Imi treatment reduced aSMase activity and ceramide content almost to the levels observed in the uninjured lung. Furthermore, aSMase activity reduction is most likely counterproductive and bears the risk of alveolar lipoproteinosis symptoms observed in experimental models of Niemann-Pick disease [58].

PIP2 compartmentalization: Compartmentalization within the airways was only proven by indirect methods assessing aSMase activity levels in BALF and in serum (Fig. 7C and D). As aSMase is present in all body fluids and tissues [27], the higher levels of activity in pulmonary tissue (Fig. 7A) and serum suggest limited epithelial penetration of PIP2 when compared to Imi.

aSMase activity: Whether reduced aSMase activity occurred as a result of suppression of activity or because of reduced gene expression by PIP2 was not assessed in our study. To the best of our knowledge aSMase gene expression studies with focus on kinetics have not been performed in clinical or experimental ALI yet. Zhang and Duan, however, showed in a cell culture study using Int407 cells subject to boswellic acid exposure that aSMase activity decreased continuously over 48 hrs, and that reduced aSMase gene expression was detectable as early as 24 hrs of incubation [59].

Decreased urine production: A S+PIP2 induced reduction in urine output was documented in our study. In a study with isolated basolateral proximal tubular cells exposed to angiotensin, activation of membrane G protein PtdIns-specific extracellular phospholipase Cβ resulted in increased Na^+-ATPase activity and hydrolysis of PtdIns-4,5-P2 to diacylglycerol and inositoltrisphosphate; Na^+-excretion (and urine production) can be blocked by inhibitors of this phospholipase Cβ or by PtdIns-4,5-P2 [60].

Conclusion

In the present neonatal triple-hit acute lung injury study we demonstrate that surfactant replacement therapy alone has no sustained effects on gas exchange, lung mechanics and pulmonary oedema. In contrast, an admixture of aSMase-inhibitors "fortifies" surfactant regardless of the more ubiquitous S+Imi effect or the compartmentalized S+PIP2 effect. Notably improved surfactant surface tensions and the lowest degree of alveolar epithelial apoptosis were observed in the S+PIP2 group, which demonstrates that cellular permeability is not necessary for the suppression of alveolar epithelial aSMase activity. As presented here for the first time, S+PIP2 treatment also suppresses gene expression of the epithelial growth factors amphiregulin and TGF-β1, and of IL-6, thus protecting the lung from pro-fibrotic stimuli during lung repair, as well as from the transpulmonary migration of monocyte-derived macrophages and granulocyates through the suppression of CD14/CD18 expression. Surfactant "fortification" by PIP2, a naturally occurring surfactant constituent, modulates inflammation at the alveolar epithelial level, is equal to Imi in terms of aSMase suppression, and exerts important additional anti-inflammatory effects. PIP2 application seems to be an interesting biological treatment concept for neonates with hypoxemic respiratory failure.

Acknowledgements

The authors thank Jürgen Hedderich, Ph.D., Institute of Medical Informatics and Statistics, for statistical advice. The surfactant preparation was generously provided by Chiesi Farmaceutici, Parma, Italy. This work was supported by a grant from Else Kröner-Fresenius-Stiftung, Bad Homburg, Germany (to M.F.K.), and by intramural funding (to M.F.K.).

Authorship

S.P., F.D.O., J.S., Sa.S., Pv.B. and M.F.K. executed the clinical experiments. S.P., Pv.B., S.U., St.S. and M.F.K. contributed to the study design. S.P., S.W.-M., S.A.-K., F.K.-L., D.L., D.W. and J.H.-F. designed the post-clinical methods and performed the analyses. M.F.K. conceived the study and wrote the first draft of the manuscript. All authors contributed to the preparation of the manuscript and approved the final version.

Conflict of interests

The authors confirm that there are no conflicts of interest.

Supporting information

Additional Supporting Information may be found in the online version of this article:

Data S1. Materials and methods.

Please note: Wiley-Blackwell are not responsible for the content or functionality of any supporting materials supplied by the authors. Any queries (other than missing material) should be directed to the corresponding author for the article.

References

1. **Husari AW, Dbaibo GS, Bitar H, *et al.*** Apoptosis and the activity of ceramide, Bax and Bcl-2 in the lungs of neonatal rats exposed to limited and prolonged hyperoxia. *Respir Res.* 2006; 7: 100/1–11.

2. **von Bismarck P, García Wistädt C-F, Klemm K, *et al.*** Improved pulmonary function by acid sphingomyelinase inhibition in a newborn piglet lavage model. *Am J Respir Crit Care Med.* 2008; 177: 1233–41.

3. **Vivekananda J, Smith D, King RJ.** Sphingomyelin metabolites inhibit sphingomyelin synthase and CTP: phosphocholine cytidylyltransferase. *Am J Physiol Lung Cell Mol Physiol.* 2001; 281: L98–107.

4. **Ryan AJ, McCoy DM, McGowan SE, *et al.*** Aleveolar sphingolipids generated in response to TNF-alpha modifies surfactant biophysical properties. *J Appl Physiol*. 2003; 94: 253–8.
5. **Göggel R, Winoto-Morbach S, Vielhaber G, *et al.*** PAF-mediated pulmonary edema: a new role for acid sphingomyelinase and ceramide. *Nat Med*. 2004; 10: 155–60.
6. **Heinrich M, Neumeyer J, Jakob M, *et al.*** Cathepsin D links TNF-induced acid sphingomyelinase to Bid-mediated caspase-9 and caspase-3 activation. *Cell Death Differ*. 2004; 11: 550–63.
7. **Chan C, Goldkorn T.** Ceramide path in human lung cell death. *Am J Respir Cell Mol Biol*. 2000; 22: 460–8.
8. **Dove SK, Johnson ZE.** Our fabulous vacation: a decade of phosphatidylinositol 3,5-bisphosphate. *Biochem Soc Symp*. 2007; 74: 129–39.
9. **Michell RH, Heath VL, Lemmon MA, *et al.*** Phosphatidylinositol 3,5-bisphosphate: metabolism and cellular functions. *Trends Biochem Sci*. 2006; 31: 52–63.
10. **Kölzer M, Arenz C, Ferlinz K, *et al.*** Phosphatidylinositol-3,5-bisphosphate is a potent and selective inhibitor of acid sphingomyelinase. *Biol Chem*. 2003; 384: 1293–8.
11. **Roth AG, Drescher D, Yang Y, *et al.*** Potent and selective inhibition of acid sphingomyelinase by bisphosphonates. *Angew Chem Int Ed*. 2009; 48: 7560–3.
12. **Krause MF, Jäkel C, Haberstroh J, *et al.*** Alveolar recruitment promotes homogeneous surfactant distribution in a piglet model of lung injury. *Pediatr Res*. 2001; 50: 34–43.
13. **Claus RA, Bunck AC, Bockmeyer CL, *et al.*** Role of increased sphingomyelinase activity in apoptosis and organ failure of patients with severe sepsis. *FASEB J*. 2005; 19: 1719–21.
14. **Tellmann G.** The E-method: a highly accurate technique for gene-expression analysis. *Nat Meth*. 2006; 3. Published online 21 June 2006. doi: 10.1038/NMETH894
15. **Wiegmann K, Schütze S, Machleidt T, *et al.*** Functional dichotomy of neutral and acidic sphingomyelinase in tumor necrosis factor signaling. *Cell*. 1994; 78: 1005–15.
16. **Jensen JM, Schütze S, Förl M, *et al.*** Roles for tumor necrosis factor receptor p55 and sphingomyelinase in repairing the cutaneous permeability barrier. *J Clin Invest*. 1999; 104: 1761–70.
17. **Henson PM, Tuder RM.** Apoptosis in the lung: induction, clearance and detection. *Am J Physiol Lung Cell Mol Physiol*. 2008; 294: L601–11.
18. **Engle WA, Committee on Fetus and Newborn**. Surfactant-replacement therapy for respiratory distress in the preterm and term neonate. *Pediatrics*. 2008; 121: 419–32.
19. **Willson DF, Thomas NJ, Markovitz BP, *et al.*** Effect of exogenous surfactant (calfactant) in pediatric acute lung injury. *JAMA*. 2005; 293: 470–6.
20. **Spragg RG, Taut FJ, Lewis JF, *et al.*** Recombinant surfactant protein C-based surfactant for patients with severe direct lung injury. *Am J Respir Crit Care Med*. 2011; 183: 1055–61.
21. **Simons K, Ikonen E.** How cells handle cholesterol. *Science*. 2000; 290: 1721–6.
22. **Kolesnick R.** The therapeutic potential of modulating the ceramide/sphingomyelin pathway. *J Clin Invest*. 2002; 110: 3–8.
23. **Prinetti A, Chigorno V, Prioni S, *et al.*** Changes in the lipid turnover, composition, and organization, as sphingolipid-enriched membrane domains, in rat cellular granule cells developing *in vitro*. *J Biol Chem*. 2001; 276: 21136–45.
24. **Longo CA, Tyler D, Mallampalli RK.** Sphingomyelin metabolism is developmentally regulated in rat lung. *Am J Respir Cell Mol Biol*. 1997; 16: 605–12.
25. **Wynn JL, Cvijanovich NZ, Allen GL, *et al.*** The influence of developmental age on the early transcriptomic response of children with septic shock. *Mol Med*. 2011; 17: 1146–56.
26. **Nussbaum C, Sperandio M.** Innate immune cell recruitment in the fetus and neonate. *J Reprod Immunol*. 2011; 90: 74–81.
27. **Takahashi I, Takahashi T, Abe T, *et al.*** Distribution of acid sphingomyelinase in human various body fluids. *Tohoku J Exp Med*. 2000; 192: 61–6.
28. **Xu Y, Seet L-F, Hanson B, *et al.*** The Phox homology (PX) domain, a new player in phosphoinositide signalling. *Biochem J*. 2001; 360: 513–30.
29. **Spyridakis S, Leondaritis G, Nakos G, *et al.*** A specific phospholipase C activity regulates phosphatidylinositol levels in lung surfactant of patients with acute respiratory distress syndrome. *Am J Respir Cell Mol Biol*. 2010; 42: 357–62.
30. **Duex JE, Nau JJ, Kauffman EJ, *et al.*** Phosphoinositide 5-phosphatase Fig 4p is required for both acute rise and subsequent fall in stress-induced phosphatidylinositol 3,5-bisphosphate levels. *Eucaryot Cell*. 2006; 5: 723–31.
31. **Bern RA, van der Loss CM, van Woensel JBM, *et al.*** Cleaved caspase-3 in lung epithelium of children who died with acute respiratory distress syndrome. *Pediatr Crit Care Med*. 2010; 11: 556–60.
32. **del Riccio V, van Tuyl M, Post M.** Apoptosis in lung development and neonatal lung injury. *Pediatr Res*. 2004; 55: 183–9.
33. **Martin TR, Hagimoto N, Nakamura M, *et al.*** Apoptosis and epithelial injury in the lungs. *Proc Am Thorac Soc*. 2005; 2: 214–20.
34. **Edwards YS, Sutherland LM, Power JHT, *et al.*** Cyclic stretch induces both apoptosis and secretion in rat alveolar type II cells. *FEBS Lett*. 1999; 448: 127–30.
35. **Kitamura Y, Hashimoto S, Mizuta N, *et al.*** Fas/FasL-dependent apoptosis of alveolar cells after lipopolysaccharide-induced lung injury in mice. *Am J Respir Crit Care Med*. 2001; 163: 762–9.
36. **Edelmann B, Bertsch U, Tchikov V, *et al.*** Caspase-8 and caspase-7 sequentially mediate proteolytic activation of acid sphingomyelinase in TNF-R1 receptosomes. *EMBO J*. 2011; 30: 379–94.
37. **Matute-Bello G, Martin TR.** Science review: apoptosis in acute lung injury. *Crit Care*. 2003; 7: 355–8.
38. **Takemura Y, Iwasaki Y, Nagata K, *et al.*** Influence of depletion of alveolar macrophages on apoptosis in Candida-induced acute lung injury. *Exp Lung Res*. 2005; 31: 307–21.
39. **Petrusca DN, Gu Y, Adamowicz JJ, *et al.*** Sphingolipid-mediated inhibition of apoptotic cell clearance by alveolar macrophages. *J Biol Chem*. 2010; 285: 40322–32.
40. **Lucas R, Verin AD, Black SM, *et al.*** Regulators of endothelial and epithelial barrier integrity and function in acute lung injury. *Biochem Pharmacol*. 2009; 77: 1763–72.
41. **Maus U, Herold S, Muth H, *et al.*** Monocytes recruited into the alveolar air space of mice show a monocytic phenotype but upregulate CD14. *Am J Physiol Lung Cell Mol Physiol*. 2001; 280: L58–68.
42. **Frevert CW, Matute-Bello G, Skerrett SJ, *et al.*** Effect of CD14 blockade in rabbits with Escherichia coli pneumonia and sepsis. *J Immunol*. 2000; 164: 5439–45.
43. **Yamamoto T, Kajikawa O, Martin TR, *et al.*** The role of leukocyte emigration and IL-8 on the development of lipopolysaccharide-induced lung injury in rabbits. *J Immunol*. 1998; 161: 5704–9.
44. **Reiss LK, Uhlig U, Uhlig S.** Models and mechanisms of acute lung injury caused by direct insults. *Eur J Cell Biol*. 2012; 91: 590–601.
45. **Dolinay T, Kaminski N, Felgendreher M, *et al.*** Gene expression profiling of target genes in ventilator-induced lung injury. *Physiol Genomics*. 2006; 26: 68–75.
46. **Spieth PM, Carvalho AR, Pelosi P, *et al.*** Variable tidal volumes improve lung protective ventilation strategies in experimental

lung injury. *Am J Respir Crit Care Med*. 2009; 179: 684–93.

47. **Chen H-H, Zhao S, Song J-G.** TGF-β1 suppresses apoptosis via differential regulation of MAP kinases and ceramide production. *Cell Death Differ*. 2003; 10: 516–27.
48. **Fahy RJ, Lichtenberger F, McKeegan CB, *et al.*** The acute respiratory distress syndrome. A role for transforming growth factor-1β. *Am J Respir Cell Mol Biol*. 2003; 28: 499–503.
49. **Budinger GRS, Chandel NS, Donnelly HK, *et al.*** Active transforming growth factor-β1 activates the procollagen I promotor in patients with acute lung injury. *Intensive Care Med*. 2005; 31: 121–8.
50. **Pekary AE, Hershman JM.** Tumor necrosis factor, ceramide, transforming growth factor-beta1, and aging reduce Na+/I-symporter messenger ribonucleic acid levels in FRTL-5 cells. *Endocrinology*. 1998; 139: 703–12.
51. **Santiago VR, Rzezinski AF, Nardelli LM, *et al.*** Recruitment maneuver in experimental acute lung injury: the role of alveolar collapse and edema. *Crit Care Med*. 2010; 38: 2207–14.
52. **Birukova AA, Tian Y, Meliton AY, *et al.*** Stimulation of Rho signaling by pathologic mechanical stretch is a "second hit" to Rho-independent lung injury induced by IL-6. *Am J Physiol Lung Cell Mol Physiol*. 2012; 302: L965–75.
53. **Peng X, Mathai SK, Murray LA, *et al.*** Local apoptosis promotes collagen production by monocyte-driven cells in transforming growth factor β1-induced lung fibrosis. *Fibrogenesis Tissue Repair*. 2011; 4: 12–25.
54. **Sparkman L, Chandru H, Boggaram V.** Ceramide decreases surfactant protein B gene expression via downregulation of TTF-1 DNA binding activity. *Am J Physiol Lung Cell Mol Physiol*. 2006; 290: L351–8.
55. **Lindner L, Uhlig U, Uhlig S.** Ceramide alters endothelial cell permeability by a nonapoptotic mechanism. *Br J Pharmacol*. 2005; 145: 132–40.
56. **Yang J, Qu J, Summah H, *et al.*** Protective effects of imipramine in murine endotoxin-induced acute lung injury. *Eur J Pharmacol*. 2010; 638: 128–33.
57. **Preuß S, Stadelmann S, Omam FD, *et al.*** Inositol-trisposphate reduces alveolar apoptosis and pulmonary edema in neonatal lung injury. *Am J Respir Cell Mol Biol*. 2012; 47: 158–69.
58. **Ikegami M, Dhami R, Schuchman EH.** Alveolar lipoproteinosis in an acid sphingomyelinase-deficient mouse model of Niemann-Pick disease. *Am J Physiol Lung Cell Mol Physiol*. 2003; 284: L518–25.
59. **Zhang Y, Duan R-D.** Boswellic acid inhibits expression of acid sphingomyelinase in intestinal cells. *Lipids Health Dis*. 2009; 8: 51.
60. **Lara LS, Correa JS, Lavelle AB, *et al.*** The angiotensin receptor type 1-Gq protein-phosphatidylinositol phospholipase Cβ-protein kinase C pathway is involved in activation of proximal tubule Na+-ATPase activity by angiotensin(1–7) in pig kidneys. *Exp Physiol*. 2008; 93: 639–47.